

Article

Study of Corrosion Resistance and Degradation Mechanisms in LiTiO₂-Li₂TiO₃ Ceramic

Dmitriy Shlimas^{1,2,*}, Artem L. Kozlovskiy^{1,2,*} and Maxim Zdorovets^{1,2,3}

¹ Laboratory of Solid State Physics, The Institute of Nuclear Physics, Almaty 050032, Kazakhstan; Shlimas@mail.ru (D.S.); mzdorovets@inp.kz (M.Z.)

² Engineering Profile Laboratory, L.N. Gumilyov Eurasian National University, Nur-Sultan 010008, Kazakhstan

³ Department of Intelligent Information Technologies, Ural Federal University, 620075 Yekaterinburg, Russia

* Correspondence: kozlovskiy.a@inp.kz; Tel.: +7-7024413368; Fax: +7-7024413368

Abstract: The interest in lithium-containing ceramics is due to their huge potential as blanket materials for thermonuclear reactors for the accumulation of tritium. However, an important factor in their use is the preservation of the stability of their strength and structural properties when under the influence of external factors that determine the time frame of their operation. This paper presents the results of a study that investigated the influence of the LiTiO₂ phase on the increasing resistance to degradation and corrosion of Li₂TiO₃ ceramic when exposed to aggressive acidic media. Using the X-ray diffraction method, it was found that an increase in the concentration of LiClO₄·3H₂O during synthesis leads to the formation of a cubic LiTiO₂ phase in the structure as a result of thermal sintering of the samples. During corrosion tests, it was found that the presence of the LiTiO₂ phase leads to a decrease in the degradation rate in acidic media by 20–70%, depending on the concentration of the phase. At the same time, and in contrast to the samples of Li₂TiO₃ ceramics, for which the mechanisms of degradation during a long stay in aggressive media are accompanied by large mass losses, for the samples containing the LiTiO₂ phase, the main degradation mechanism is pitting corrosion with the formation of pitting inclusions.

Keywords: Li₂TiO₃; blanket materials; corrosion; degradation; strength



Citation: Shlimas, D.; Kozlovskiy, A.L.; Zdorovets, M. Study of Corrosion Resistance and Degradation Mechanisms in LiTiO₂-Li₂TiO₃ Ceramic. *Crystals* **2021**, *11*, 753. <https://doi.org/10.3390/cryst11070753>

Academic Editor: Vladislav V. Khartov

Received: 13 June 2021
Accepted: 25 June 2021
Published: 27 June 2021

Publisher's Note: MDPI stays neutral with regard to jurisdictional claims in published maps and institutional affiliations.



Copyright: © 2021 by the authors. Licensee MDPI, Basel, Switzerland. This article is an open access article distributed under the terms and conditions of the Creative Commons Attribution (CC BY) license (<https://creativecommons.org/licenses/by/4.0/>).

1. Introduction

For fusion reactors, one of the important operating conditions is the production and subsequent accumulation of tritium to maintain the stable operation of the reactor. At the same time, due to the low presence of tritium in its natural form, reactions of tritium multiplication under the action of neutron fluxes have been proposed for thermonuclear reactors. The most energetically advantageous nuclear reaction for lithium accumulation is ${}^6\text{Li} + n \rightarrow {}^4\text{He} + \text{T} + 4.8 \text{ MeV}$ reaction, which allows not only the obtaining of tritium, but also the generation of a large amount of energy [1–3]. One of the most promising materials for such reactions are lithium-containing ceramics such as Li₂TiO₃, Li₄SiO₄, Li₂ZrO₃, etc., which not only have good mechanical properties, but also contain a large amount of lithium [4–6]. At the same time, it was shown in a number of works that the presence of two-phase ceramics of Li₂TiO₃-Li₄SiO₄ or LiTiO₂-Li₂TiO₃ type leads not only to an increase in the strength of the ceramics, but also significantly affects the yield of tritium and its resistance to radiation damage arising during the accumulation of lithium [7–10]. The presence of a “core-shell” structure in such ceramics opens up wide possibilities for the production of tritium, as well as for high mechanical strength. However, despite the great prospects for using these lithium-containing ceramics as materials for tritium breeders, today there is little experimental data on the resistance of ceramics to degradation, and in particular, to the effect of aggressive media. As is known, corrosion processes, which are accompanied by the introduction of oxygen with the subsequent formation of amorphous inclusions or areas of disorder, can lead to significant consequences in the

performance of materials. Thus, for example, in works [11,12] devoted to the study of the processes of tritium release from their $\text{Li}_2\text{TiO}_3\text{-Li}_4\text{SiO}_4$ ceramic, it was found that structural defects that accumulate in the material under the action of irradiation make a significant contribution to the production of lithium. The presence of structural defects can lead to the formation of a large number of disordering regions, as well as to a significant increase in the porosity of ceramics, which leads to their degradation and, consequently, to a decrease in the yield of tritium [11–15]. At the same time, data on degradation resistance of lithium-containing ceramics under the action of ionizing radiation indicates a high radiation resistance of ceramics [16–20]; however, such data on corrosion resistance in aggressive media, such as acids or alkalis, are insufficient. The lack of objective data on the processes of corrosion and degradation in corrosive media opens up broad prospects for researchers to conduct such experiments. Interest in them is due to the possibility of obtaining kinetic curves of the degradation rate, which in the future will make it possible to contribute to the characterization of lithium-containing ceramics for thermonuclear power engineering [21–25]. Also of particular interest is the study of the effect of the presence of two-phase structures on resistance to degradation, since earlier studies indicate that two-phase ceramics have higher strength and durability [25–27].

Based on the above, the main purpose of this work was to study the effect of the LiTiO_2 phase on increasing the resistance to degradation and corrosion of Li_2TiO_3 ceramic exposed to aggressive acidic and alkaline media.

2. Experimental Part

The preparation of lithium-containing ceramics was carried out using the method of solid-phase synthesis in various stoichiometric ratios of TiO_2 and $\text{LiClO}_4 \cdot 3\text{H}_2\text{O}$ (99.99% Sigma–Aldrich, Saint Louis, MO, USA) salts. Solid-phase synthesis was carried out by mixing TiO_2 and $\text{LiClO}_4 \cdot 3\text{H}_2\text{O}$ salts into tungsten carbide glasses in a planetary mill at a grinding speed of 400 rpm for 1 hour, followed by thermal annealing of the resulting mixture in a muffle furnace at 1000 °C for 5 hours. Thermal annealing was carried out in an isochronous mode, followed by cooling of the resulting mixture together with the furnace for 24 hours. The stoichiometric ratios of TiO_2 and $\text{LiClO}_4 \cdot 3\text{H}_2\text{O}$ salts for three samples were selected in the following ratio: Sample 1 (LTO-1) 0.9M TiO_2 and 0.1M $\text{LiClO}_4 \cdot 3\text{H}_2\text{O}$; Sample 2 (LTO-2) 0.7M TiO_2 and 0.3M $\text{LiClO}_4 \cdot 3\text{H}_2\text{O}$; Sample 3 (LTO-3) 0.5M TiO_2 and 0.5M $\text{LiClO}_4 \cdot 3\text{H}_2\text{O}$.

Characterization of the morphological features of the samples was carried out using a scanning electron microscopy method performed on a JEOL 7500F microscope (JEOL, Tokyo, Japan).

The study of the dynamics of structural parameters change was carried out using the method of X-ray diffraction, implemented on an X-ray diffractometer D8 Advance Eco (Bruker, Berlin, Germany). X-ray photography was carried out in the Bregg–Brentano geometry in the angular range $2\theta = 25\text{--}85^\circ$, with a step of 0.03° and a spectrum acquisition time at a point of 1 second.

Corrosion tests were carried out using an acid solution. A 20% sulfuric acid model solution was used as the acid solution. The choice of this acid concentration was due to the ability to model most aggressive acid media used as electrolyte solutions. The time range of measurements was 30 days, measurements of structural and dielectric characteristics were carried out every 3 days. The test temperature was 25, 50, and 75 °C. The tests were carried out by placing the samples in a beaker with a sulfuric acid solution, so that the whole sample was placed in an acid covered with a lid, once placed on a heating device that maintained a constant temperature of the medium. The mass loss was measured as follows: after a certain period of time, the acid solution was gently drained into the tank, and the samples were weighed on the analytical scales after a short hold for drying. Mass loss measurements were taken in five parallels to obtain statistical data.

Destruction resistance measurements of ceramic were carried out by single compression in a special mold with a compression rate of 0.1 mm per minute.

3. Results and Discussion

Figure 1 shows X-ray diffraction patterns of the synthesized samples depending on the composition. The general view of the diffraction patterns indicates the polycrystalline structure of the synthesized ceramic, while a change in stoichiometry leads to the formation of new peaks, which indicates that a new phase was formed in the structure of the ceramic. According to the phase analysis performed, it was found that for the LTO-1 sample, the angular position and intensities of diffraction reflections corresponded to the monoclinic phase Li_2TiO_3 with the crystal lattice parameters $a = 5.042 \text{ \AA}$, $b = 8.741 \text{ \AA}$, $c = 9.717 \text{ \AA}$, $\beta = 100.15^\circ$. For samples LTO-2 and LTO-3, the observed appearance of new diffraction reflections corresponded to the formation of the cubic phase of LiTiO_2 . Moreover, in the case of the LTO-3 sample, this phase was well structured, in contrast to the LTO-2 sample. The formation of the cubic phase in the samples led to a change in the parameters of the crystal lattice due to the processes of phase formation. Thus, the parameters of the crystal lattices for the LTO-2 sample, according to estimates, were for the monoclinic phase Li_2TiO_3 $a = 5.010 \text{ \AA}$, $b = 8.703 \text{ \AA}$, $c = 9.679 \text{ \AA}$, $\beta = 99.84^\circ$, for the cubic phase LiTiO_2 $a = 8.4596 \text{ \AA}$. For the LTO-3 sample, for the monoclinic phase Li_2TiO_3 $a = 4.991 \text{ \AA}$, $b = 8.681 \text{ \AA}$, $c = 9.662 \text{ \AA}$, $\beta = 99.94^\circ$, for the cubic phase LiTiO_2 $a = 8.478 \text{ \AA}$. Using full-profile analysis to estimate the peak areas and formula $V_{\text{admixture}} = \frac{RI_{\text{phase}}}{I_{\text{admixture}} + RI_{\text{phase}}}$, where I_{phase} is the average integrated intensity of the main phase of the diffraction line, $I_{\text{admixture}}$ is the average integrated intensity of the additional phase, and R is the structure coefficient equal to 1.45, the ratios of the contributions of the two phases were determined for the LTO-2 and LTO-3 samples. The $\text{Li}_2\text{TiO}_3/\text{LiTiO}_2$ phase ratio for the LTO-2 and LTO-3 samples was 91/9 and 79/21, respectively. Using the formula $\text{Crystallinity} = \frac{S_{\text{cr}}}{S_{\text{cr}} + S_{\text{am}}} * 100\%$, where S_{cr} is the area of diffraction reflections, S_{am} is the area characteristic of disordered regions or an amorphous halo, the degree of crystallinity was determined, which characterizes the structural ordering as a result of the processes of structure formation during synthesis and phase formation. According to the data obtained, the crystallinity degree for the samples under study was 89.5–91%, which indicates a high degree of structural ordering. The formation of the cubic phase, according to the analysis of the density of ceramic from the obtained X-ray diffraction data, leads to its increase from 3.459 g/cm^3 for the LTO-1 sample, to 3.536 g/cm^3 and 3.581 g/cm^3 for the LTO-2 and LTO-3 samples, respectively. Thus, it was found that an increase in the contribution of the cubic phase of LiTiO_2 leads not only to an increase in the degree of structural ordering and density of ceramic, but also to a decrease in porosity, which significantly affects the strength properties of ceramic. To calculate porosity, a method based on a change in ceramic density obtained from the analysis of the crystal lattice volume change was used. As the calculation formula, $P_{\text{dil}} = (1 - \frac{\rho}{\rho_0}) * 100\%$ was used, where ρ_0 is the density of the reference sample. According to the calculations, the porosity of the LTO-1, LTO-2, and LTO-3 samples was 6.5%, 4.8%, and 3.2%, respectively.

Figure 2 shows the results of changes in morphological features of the synthesized ceramics, depending on the change in composition. From the presented data, it can be seen that, for the LTO-1 sample, small pyramidal or rhomboid particles predominate, the average size of which varies from 30 to 50 nm. There are also large pyramidal particles in the structure, the concentration of which does not exceed 5–10% of the total. In the case when a cubic phase begins to form in the structure of ceramic, an enlargement of the particle size during sintering is observed, as well as a change in their shape from rhomboid and pyramidal to close to spherical or oval. There is also an increase in particle sizes to 100–120 nm and 150–200 nm in the cases of samples LTO-2 and LTO-3, respectively. This behavior indicates that the formation of the cubic phase of LiTiO_2 in the structure of ceramic has a significant effect on the morphological features of particles. It can also be seen from a detailed analysis of the morphological features that an increase in the LiTiO_2 phase leads not only to an enlargement of particles, but also to their compaction with the formation of large agglomerates fused together, in contrast to LTO-1 samples, for which the upper layer of particles appears loose and porous.

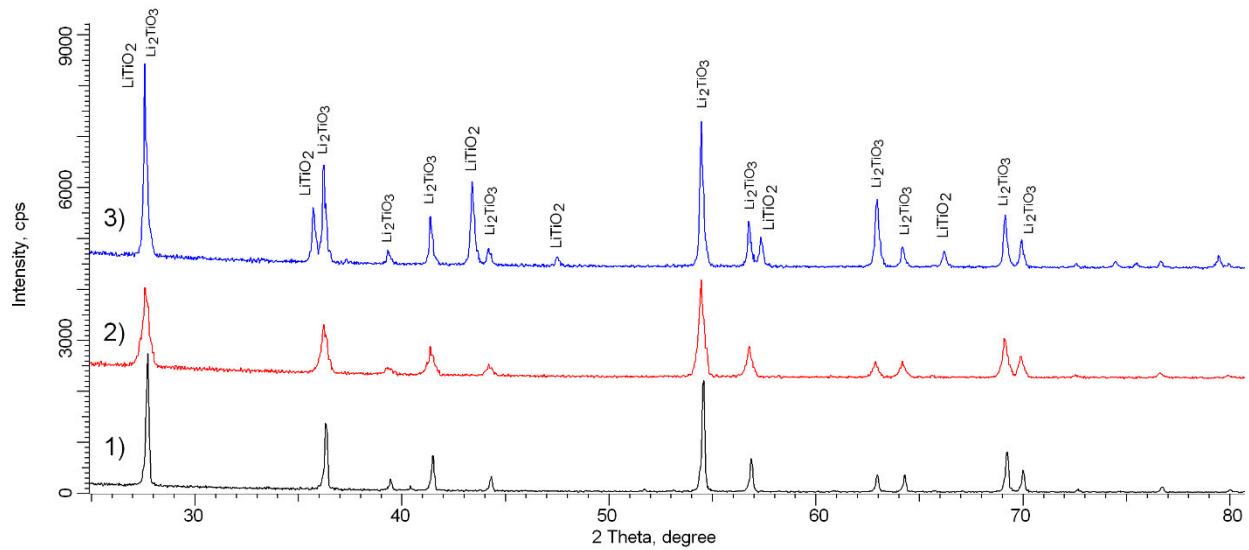


Figure 1. X-ray diffraction patterns of the samples under study: 1) LTO-1; 2) LTO-2; 3) LTO-3.

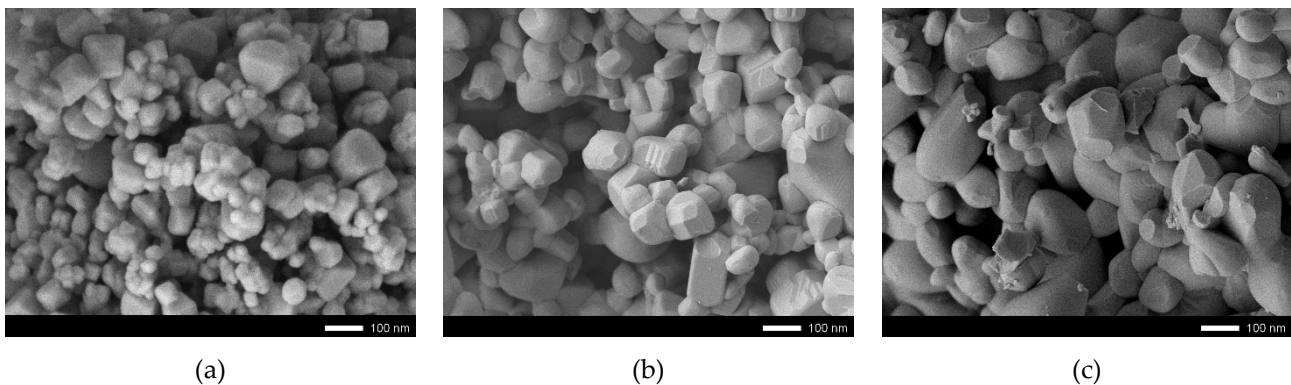


Figure 2. SEM images of synthesized ceramics: (a) LTO-1; (b) LTO-2; (c) LTO-3.

As is known, lithium and titanium belong to a group of metals of increased instability, which means that they can corrode in neutral media by oxidation and amorphization. This behavior of these structures makes them unstable to external influences, which can significantly affect the performance of ceramics when interacting with the environment. At the same time, an important role in the assessment of corrosion processes is played by such quantities as the loss or increase in mass of the samples, as well as the corrosion rate, which is determined by a whole set of factors, such as the phase composition, surface morphology, the degree of structural perfection in the initial state, etc.

Figure 3 shows the results of changes in the mass of samples during corrosion tests in an acidic electrolyte, depending on the temperature of the environment. The general view of the changes is characterized by two stages, which reflect different degradation processes. The first stage is characterized by an insignificant mass gain of 1.5–2.0%, which is associated with the formation of an oxide film on the surface of ceramics. In this case, the time frames for this stage were different for both the solution temperature and the type of ceramics. For example, the weight gain for LTO-1 samples occurs in the range of 5 to 15 days, depending on the temperature of the electrolyte. It was also found that an increase in the electrolyte temperature leads to a decrease in the time interval for weight gain, which indicates an increase in the rate of degradation. For samples LTO-2 and LTO-3, the processes of weight gain begin after 6–10 days of being in solution, which indicates resistance to the formation of oxide films on ceramics. In this case, in the case of the LTO-3

sample, the time of formation of an oxide film and an increase in mass at an electrolyte temperature of 25 °C occurred after 20 days of being in the electrolyte.

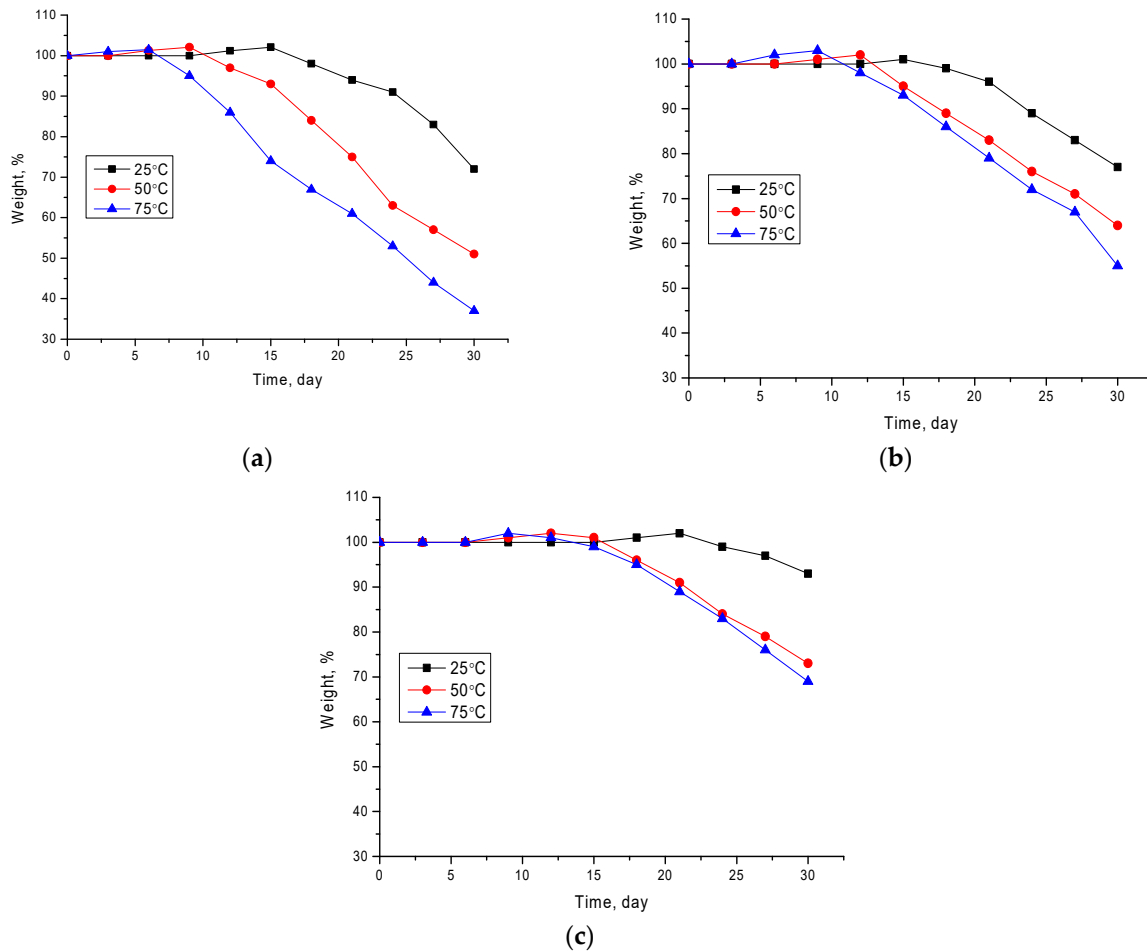


Figure 3. Graph of changes in the mass of ceramics depending on the time spent in the medium: (a) LTO-1; (b) LTO-2; (c) LTO-3.

The second stage is characterized by a decrease in mass, which is due to the occurrence of degradation and corrosion processes associated with the formation of amorphous inclusions and partial destruction of the samples. In this case, as for all the samples under study, there was a tendency to increase in weight loss, with an increase in the electrolyte temperature. This behavior of corrosion processes is due to the acceleration of the dissolution of the formed oxide film at the initial stage, followed by the introduction of oxygen and hydrogen into the structure, leading to the destruction of chemical and crystalline bonds. In this case, the most probable processes are pitting corrosion or intergranular corrosion occurring at grain boundaries. In the case of LTO-1 samples, for which, in the initial state, a porous layer on the surface of the particles was observed on the surface, the rate of weight loss is maximum, and the maximum losses were from 30 to 60% of the initial weight, depending on the electrolyte temperature. At the same time, in the case of samples LTO-2 and LTO-3, the mass loss was much less. Such a difference in the dynamics of mass change for samples LTO-2 and LTO-3 compared to sample LTO-1 may be associated with the presence of a cubic phase in their structure, as well as larger particle sizes, in addition to a decrease in the concentration of porous inclusions in the structure due to higher density.

Based on the obtained data on the change in the mass of ceramics, the specific corrosion rate was calculated using the formula $\vartheta = \frac{\Delta m}{S \cdot t}$, where Δm is the change in the mass of the samples, S is the surface area, and t is the corrosion time. Figure 4a shows the calculation results. As can be seen from the presented data, the largest decrease in the corrosion rate

was observed for the LTO-3 samples, for which the decrease in the corrosion rate was from 50 to 70%. This decrease was due to the presence of a cubic phase in the structure, which, as mentioned earlier, leads to a strengthening of the structure and a decrease in the corrosion rate. At the same time, an increase in temperature leads to a sharp increase in the rate of degradation of the surface layer, which indicates the instability of single-phase structures to aggressive media at elevated temperatures. The formation of a cubic phase and an increase in its concentration leads to a significant decrease in the degradation rate, which indicates an increase in the ceramic stability.

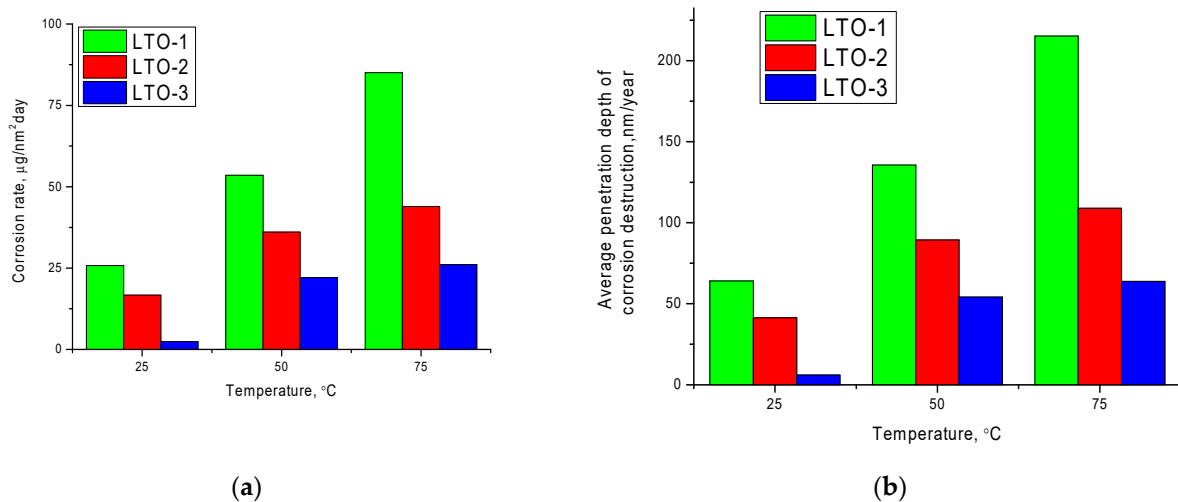
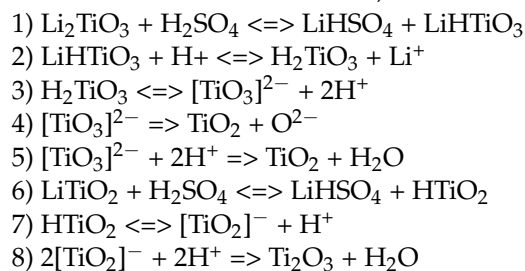


Figure 4. (a) Graph of changes in the specific corrosion rate; (b) Graph of changes in average depth of corrosion penetration.

Figure 4b shows the results of the change in the depth corrosion value of the ceramics surface obtained, taking into account the density change data. From the data presented, it can be seen that the formation of the LiTiO_2 cubic phase, resulting in an increase in the density of the ceramics, had a significant effect on the depth of the corrosive layer over time. A two- to three-fold decrease in the depth of corrosion for samples LTO-2 and LTO-3, in comparison with sample LTO-1 at high temperatures of an aggressive medium, was due to the denser ceramic surface structure, as well as low density. In the case of LTO-3 samples, when they were in an aggressive environment at a temperature of 25 °C, the low corrosion rate and the depth of the corroded surface indicates that the main corrosion mechanism in this case was pitting and intergranular corrosion, which is clearly seen on the SEM images of LTO-3 samples after 30 days of testing (See Figure 5). Figure 5 also shows the results of elemental analysis performed from different parts of the samples with significant visual differences (marked with orange circles). According to the elemental analysis, the regions without porous inclusions contained 24–25 at.% titanium and 74–75 at.% oxygen (lithium is a forbidden element for the energy dispersive analysis method). This ratio of titanium and oxygen elements was close enough for the stoichiometric ratio $\text{Ti}:\text{O} = 1:3$. The porous areas marked in Figure 5 by points 3–5, according to the elemental analysis data, contained a higher oxygen content of 80–82%, which indicates that degradation occurs due to the formation of porous inclusions containing a high oxygen concentration. When ceramics react with a solution of sulfuric acid, the following chemical reactions (1–8) are possible:



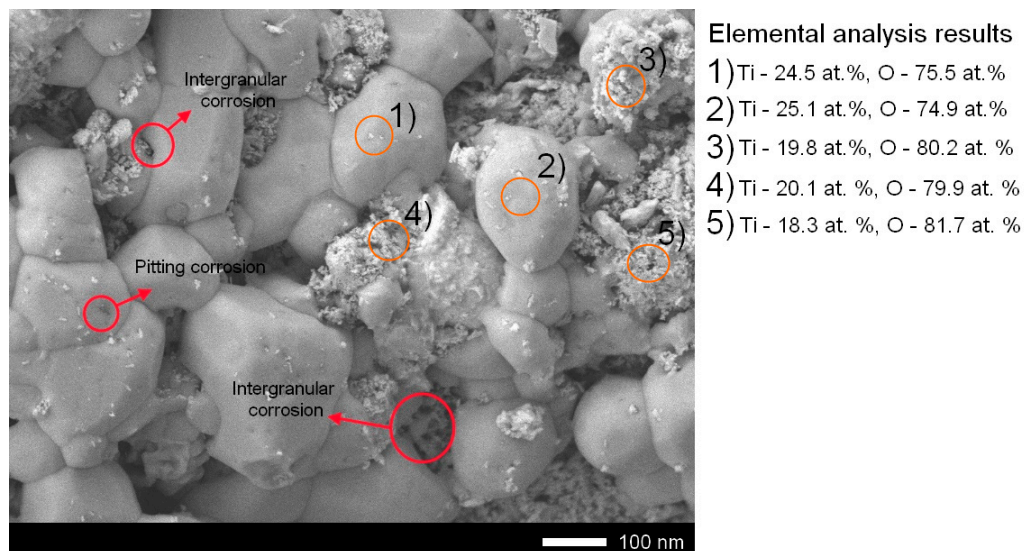


Figure 5. Corrosion results of LTO-3 sample after 30 days of testing.

When Li_2TiO_3 and LiTiO_2 react with sulfuric acid, lithium ion is first exchanged for hydrogen ion to form completely substituted phases. Therefore, high acidity can lead to the release of oxygen and the formation of titanium oxides. However, as the X-ray phase analysis shows, no titanium oxides were detected on the samples, thus most likely only 20% sulfuric acid is not sufficient for 4,5 reactions to take place in the case of Li_2TiO_3 and reaction 8 in the case of LiTiO_2 . Thus, etching occurs, followed by destruction of the particles under the influence of acid. Since the structure of Li_2TiO_3 has cavities due to the monoclinic structure, the Li_2TiO_3 etching reaction rate is higher than in the case of a cubic, denser structure of LiTiO_2 .

Figure 6 shows the results of X-ray diffraction of the samples under study after corrosion tests at a temperature of 75 °C. As can be seen from the data presented, the main structural changes are associated with deformation and changes in diffraction reflection intensities of the samples in comparison with the initial X-ray diffraction patterns. At the same time, the formation of new peaks was not established, which indicates the absence of phase transformation processes, or may be due to the washing out of the formed metastable phases in the near-surface damaged layer during the tests. Moreover, the main changes included the ratio of areas characteristic of amorphous inclusions and diffraction reflections, which characterizes the structural ordering degree (crystallinity degree). As can be seen from the data presented, the LTO-1 sample, for which the greatest changes in diffraction reflections are observed, associated with an increase in shape asymmetry and a sharp decrease in reflections intensity, while the decrease in crystallinity degree of was more than 40% (from 89.5% to 46.7%). At the same time, the shape of the main reflections at $2\theta = 28$ and 36° was sharply deformed with the formation of a halo-like structure, which indicates strong amorphization. In the case of two-phase LTO-2 and LTO-3 samples, changes in the intensities and shapes of diffraction reflections were less pronounced. At the same time, in the case of the LTO-3 sample, the main changes are associated with the reflection intensities ratio redistribution characteristic of the Li_2TiO_3 and LiTiO_2 phases. The change in the ratio indicates that the amorphization of the structure occurs as a result of the decomposition of the Li_2TiO_3 phase, the reflection intensities of which become lower in comparison with the reflection intensities characteristic of the LiTiO_2 phase. At the same time, for the LTO-3 sample, the deformation of the reflections shape was less pronounced than for other samples, which indicates a lower degradation degree and a lower corrosion rate. The analysis of changes in the porosity of samples after corrosion tests in comparison with the initial data is shown in Figure 7. The data presented shows that, as a result of corrosion tests, the greatest change in porosity was observed for LTO-1 samples, for which the increase in porosity was 2.2–2.8 times, depending on the medium temperature. In this

case, for LTO-3 samples, the change in porosity was no more than 62.5% at a temperature of 75 °C, which indicates a high degradation resistance of ceramics.

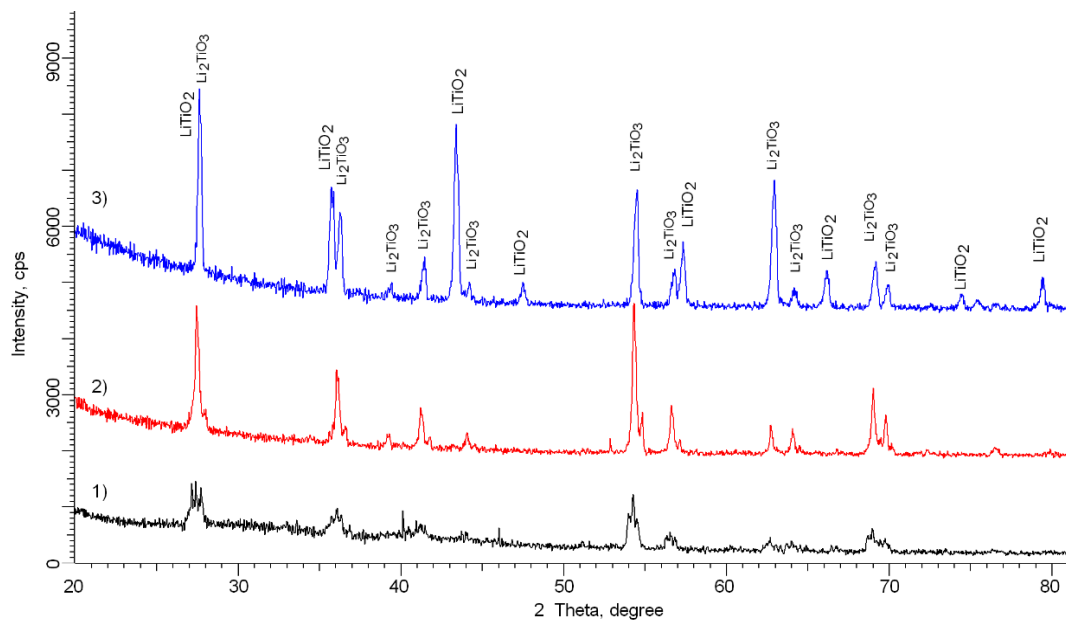


Figure 6. X-ray diffraction patterns of the test samples after corrosion tests at 75 °C: 1) LTO-1; 2) LTO-2; 3) LTO-3.

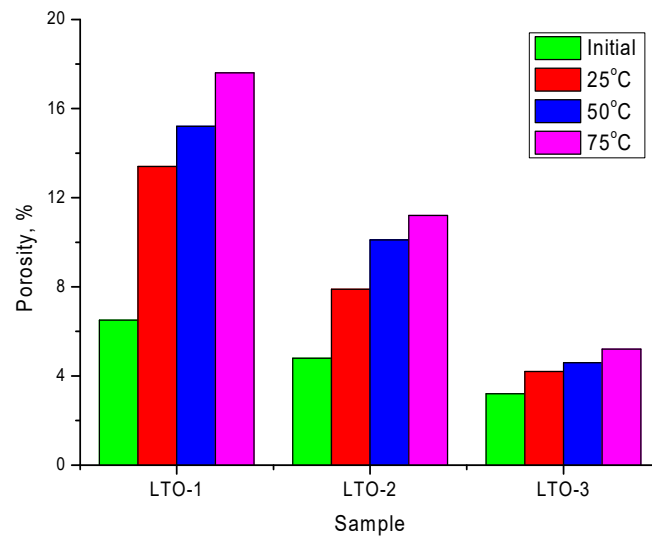


Figure 7. Results of change in ceramic porosity depending on exposure conditions.

In the case of a large loss of sample mass during a long-term corrosion process, the main degradation mechanisms are the formation of amorphous inclusions and disordering regions, which lead to a sharp increase in deformation distortions in the structure and subsequent destruction of crystalline and chemical bonds. The deformation of the crystal structure can be caused both by the processes of incorporation of oxygen and hydrogen, and due to the formation of transient metastable oxide phases of titanium or lithium, leading to partial destruction of the structure. Based on the analysis of changes in the parameters of the crystal lattice, interplanar distances, the indices of the degree of deformation of the crystal lattice, were calculated for all the samples under study, depending on the conditions of being in the medium. The deformation index characterizes the stability of the crystal structure to external influences, and can serve as a measure for determining the critical point, after which the structure of ceramics breaks down and degrades. The results of

the change in the deformation index are shown in Figure 8. The deformation index was calculated based on the change in the diffraction maxima position, characterizing the interplanar distance. For calculations, the following formula was used: $\varepsilon = \frac{d_{corr} - d_{pristine}}{d_{pristine}}$, where $d_{pristine}$, d_{corr} are interplanar distances before and after external influences.

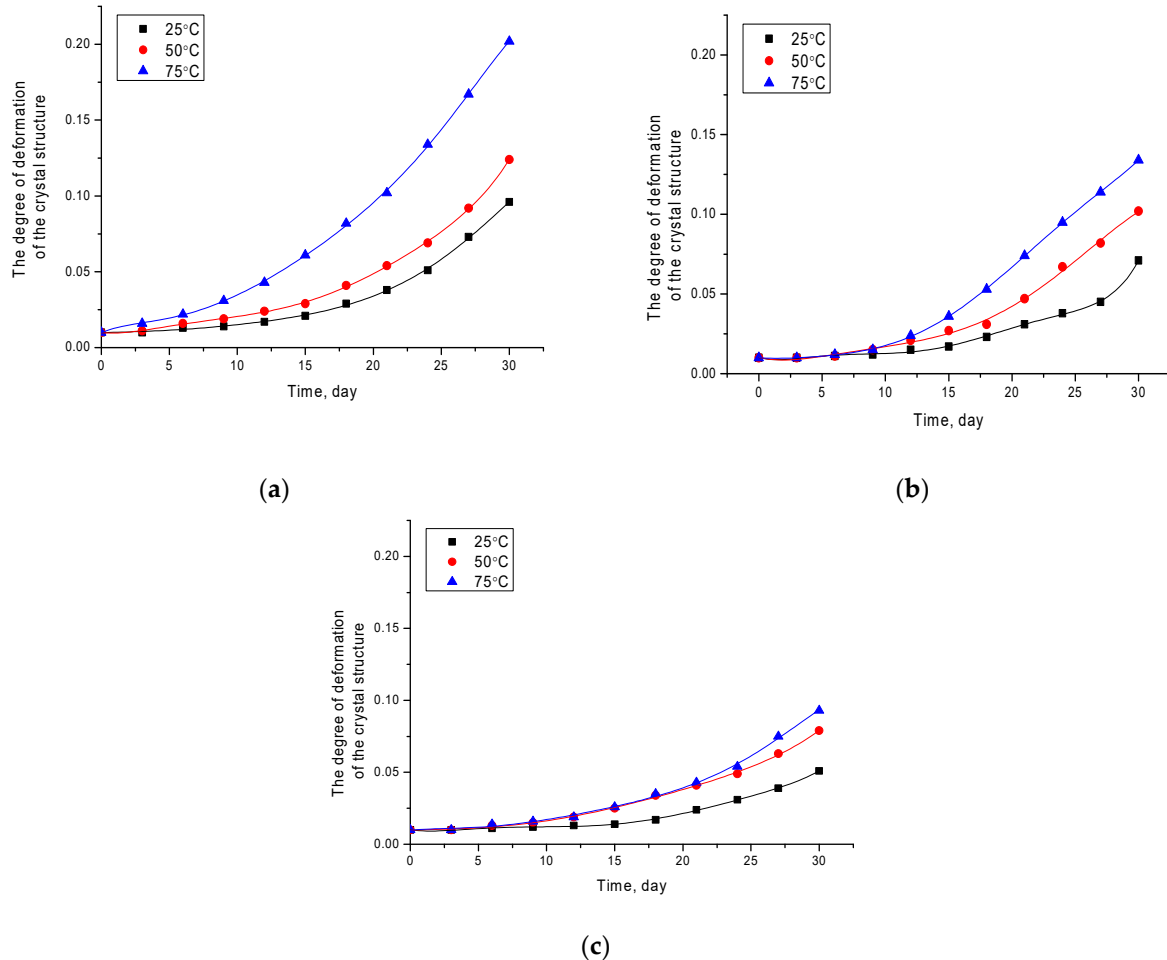


Figure 8. Graph of the change in the deformation degree of the crystal structure depending on the time spent in medium: (a) LTO-1; (b) LTO-2; (c) LTO-3.

The results obtained clearly confirm the previously stated assumption that, at high mass losses, the crystal structure is deformed due to the formation of amorphous inclusions and disordering, leading to the destruction of ceramics. Therefore, for the LTO-1 samples for which the maximum weight loss was observed, the degree of deformation of the crystal structure is maximum. At the same time, the nature of the change in the magnitude of the degree of deformation is exponential, characterized by two stages of change. The first stage of changing the degree of deformation of the crystal structure for all samples consists in small changes in the value and varies from 10 to 15, or 15 to 20, days, depending on the phase composition of the samples. This period coincides with the period for which the formation of oxide films on the surface of ceramics, characterized by an increase in mass, is characteristic. At this stage, small changes in the degree of deformation are due to the low rate of introduction of oxygen and hydrogen ions into the interstices of the crystal lattice of the near-surface layer of ceramics. The onset of degradation processes associated with the loss of mass due to the partial destruction of the structure and its amorphization is accompanied by a sharp exponential increase in the degree of deformation of the crystal structure. At the same time, for LTO-3 samples, for which it was found that the main degradation mechanisms are associated with pitting and intergranular corrosion,

the maximum degradation degree was 0.05–0.09, depending on the temperature of the medium, while a similar value for LTO-1 samples was approximately 1.5–2 times more.

Another important factor influencing the assessment of the use of ceramics under the influence of this environment is the resistance of the strength properties of ceramics to crack and fracture resistance. Earlier in [28], it was shown that the formation of a cubic phase in the structure of ceramics leads to an increase in resistance to cracking from 23 N to 40–43 N. At the same time, an increase in stability was associated with an increase in the density and degree of the crystallinity of ceramics. Figure 9 shows a graph of changes in fracture resistance in both the initial state and after 10, 20, and 30 days of corrosion tests.

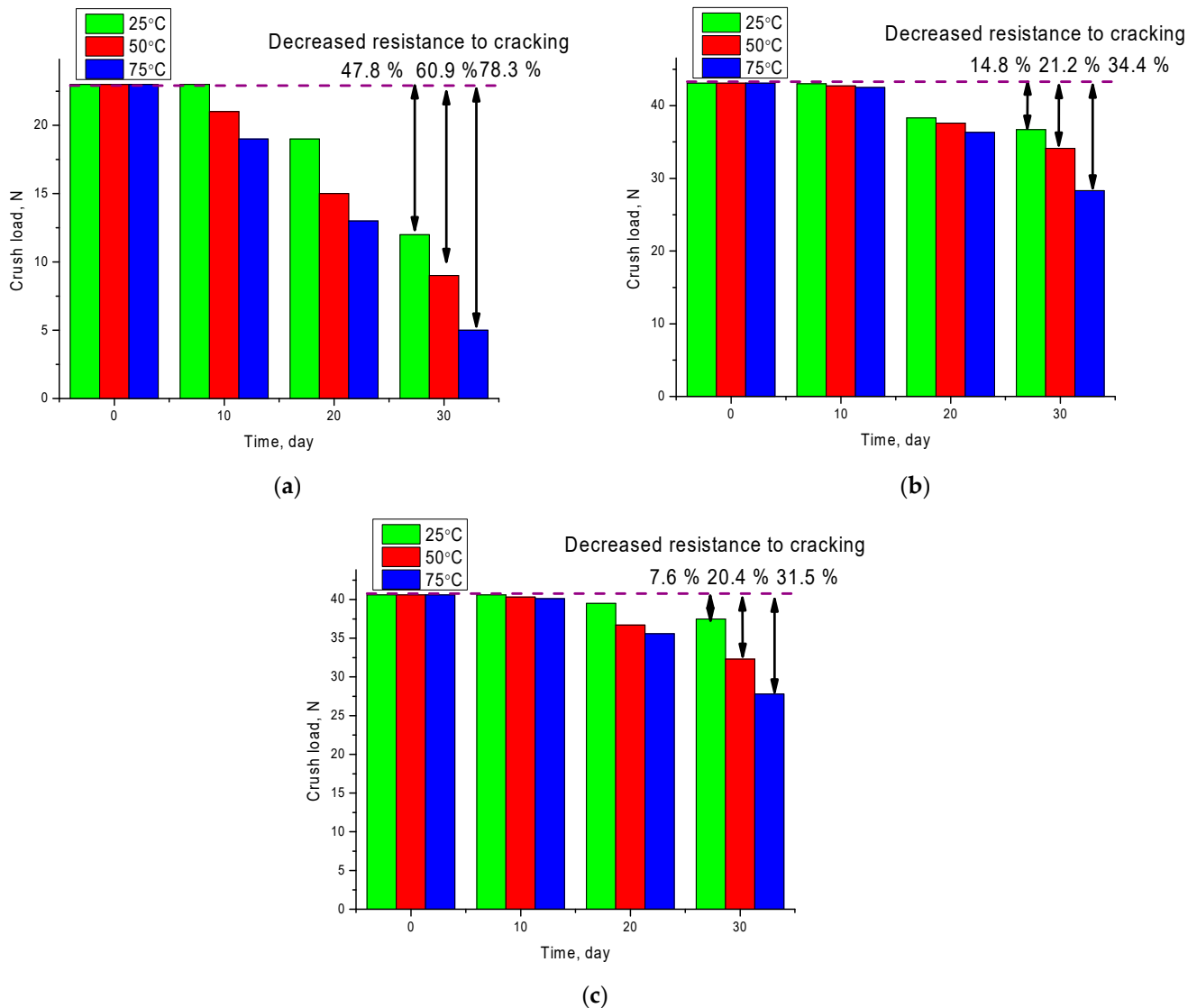


Figure 9. Graph of changes in ceramics fracture resistance: (a) LTO-1; (b) LTO-2; (c) LTO-3.

According to the data obtained, corrosion processes accompanied by mass loss and deformation of the crystal structure lead to a sharp decrease in ceramics resistance to cracking and destruction. In this case, the maximum decrease in fracture toughness for LTO-1 samples was from 47 to 78%, depending on the solution temperature. For two-phase samples LTO-2 and LTO-3, the maximum decrease in resistance to cracking and fracture was no more than 32%, which is more than 1.5–2 times less than similar indicators for LTO-1 samples. At the same time, in the case of the LTO-3 sample, when it was in an environment at a temperature of 25 °C, the maximum decrease in the resistance value was

no more than 8%, which indicates a high degree of ceramics resistance to degradation and destruction as a result of external pressure forces.

Thus, summarizing all of the above, we can conclude that the formation of two-phase LiTiO_2 - Li_2TiO_3 ceramics with a cubic phase content of no more than 10–20% can significantly increase both the strength properties of ceramics and increase the resistance to degradation and corrosion, as well as reduce the oxidation and destruction rate of ceramics. The results obtained are also in good agreement with other works [9–14] devoted to studying the effect of two phases on the stability of lithium-containing ceramics and increasing the efficiency of their productivity.

4. Conclusions

This paper presents the results of a study investigating the effect of the LiTiO_2 phase on increasing the resistance to degradation and corrosion of Li_2TiO_3 ceramic exposed to aggressive acidic media. Using the X-ray phase analysis method, it was found that the formation of the cubic phase increased from 3.459 g/cm^3 for sample LTO-1, to 3.536 g/cm^3 and 3.581 g/cm^3 for samples LTO-2 and LTO-3, respectively. It was also determined that an increase in the contribution of the cubic phase of LiTiO_2 leads not only to an increase in the degree of structural ordering and density of ceramics, but also to a decrease in porosity, which significantly affects the strength properties of ceramics.

During corrosion tests, it was found that a two- to three-fold decrease in the depth of corrosion for samples LTO-2 and LTO-3, in comparison with sample LTO-1 at high temperatures of an aggressive environment, is due to the denser structure of the ceramic surface, as well as low density. At the same time, for LTO-3 samples, when they are in an aggressive environment at a temperature of $25 \text{ }^\circ\text{C}$, the low corrosion rate and the depth of the corroded surface indicate that the main corrosion mechanism in this case is pitting and intergranular corrosion.

The results of further work can be used in assessing the applicability of lithium-containing ceramics, not only as blanket materials, but also as a basis for lithium-ion anode materials.

Author Contributions: Data curation, D.S.; Formal analysis, D.S.; Investigation, A.L.K. and M.Z.; Resources, M.Z.; Visualization, A.L.K.; Writing—original draft, A.L.K. All authors have read and agreed to the published version of the manuscript.

Funding: This research was funded by the Science Committee of the Ministry of Education and Science of the Republic of Kazakhstan (No. AP08855734).

Institutional Review Board Statement: Not applicable.

Informed Consent Statement: Not applicable.

Data Availability Statement: Not applicable.

Conflicts of Interest: The authors declare no conflict of interest.

References

1. Hoshino, T.; Edao, Y.; Kawamura, Y.; Ochiai, K. Pebble fabrication and tritium release properties of an advanced tritium breeder. *Fusion Eng. Des.* **2016**, *109*, 1114–1118. [[CrossRef](#)]
2. Roux, N.; Avon, J.; Floreancing, A.; Mougin, J.; Rasneur, B.; Ravel, S. Low-temperature tritium releasing ceramics as potential materials for the ITER breeding blanket. *J. Nucl. Mater.* **1996**, *233*, 1431–1435. [[CrossRef](#)]
3. Uchida, M.; Ishitsuka, E.; Kawamura, H. Tritium release properties of neutron-irradiated Be_{12}Ti . *J. Nucl. Mater.* **2002**, *307*, 653–656. [[CrossRef](#)]
4. Munakata, K.; Yokoyama, Y.; Baba, A.; Kawagoe, T.; Takeishi, T.; Nishikawa, M.; Penzhorn, R.D.; Moriyma, H.; Kawamoto, K.; Morimoto, Y.; et al. Tritium release from catalytic breeder materials. *Fusion Eng. Des.* **2001**, *58*, 683–687. [[CrossRef](#)]
5. Kolb, M.; Bruns, M.; Knitter, R.; van Til, S. Lithium orthosilicate surfaces: Characterization and effect on tritium release. *J. Nucl. Mater.* **2012**, *427*, 126–132. [[CrossRef](#)]
6. Kwast, H.; Conrad, R.; Kennedy, P.; Flipot, A.; Elen, J. In-pile tritium release from LiAlO_2 , Li_2SiO_3 and Li_2O in EXOTIC experiments 1 and 2. *J. Nucl. Mater.* **1986**, *141*, 300–304. [[CrossRef](#)]

7. Hoshino, T. Pebble fabrication of super advanced tritium breeders using a solid solution of $\text{Li}_{2+x}\text{TiO}_{3+y}$ with Li_2ZrO_3 . *Nuclear Mater. Energy* **2016**, *9*, 221–226. [[CrossRef](#)]
8. Ran, G.; Xiao, C.; Chen, X.; Gong, Y.; Zhao, L.; Wang, H.; Wang, X. Tritium release behavior of Li_4SiO_4 pebbles with high densities and large grain sizes. *J. Nucl. Mater.* **2017**, *492*, 189–194. [[CrossRef](#)]
9. Yang, M.; Zhao, L.; Ran, G.; Gong, Y.; Wang, H.; Peng, S.; Xiao, C.; Chen, X.; Lu, T. Tritium release behavior of Li_2TiO_3 and $2\text{Li}_2\text{TiO}_3\text{-Li}_4\text{SiO}_4$ biphasic ceramic pebbles fabricated by microwave sintering. *Fusion Eng. Des.* **2021**, *168*, 112390. [[CrossRef](#)]
10. Xiang, M.; Zhang, Y.; Zhang, Y.; Liu, S.; Liu, H.; Wang, C.; Gu, C. Preparation of $\text{Li}_2\text{TiO}_3\text{-Li}_4\text{SiO}_4$ core-shell ceramic pebbles with enhanced crush load by graphite bed process. *J. Nucl. Mater.* **2015**, *466*, 477–483. [[CrossRef](#)]
11. Yang, M.; Ran, G.; Wang, H.; Dang, C.; Huang, Z.; Chen, X.; Lu, T.; Xiao, C. Fabrication and tritium release property of $\text{Li}_2\text{TiO}_3\text{-Li}_4\text{SiO}_4$ biphasic ceramics. *J. Nucl. Mater.* **2018**, *503*, 151–156. [[CrossRef](#)]
12. Zhou, Q.; Togari, A.; Nakata, M.; Zhao, M.; Sun, F.; Xu, Q.; Oya, Y. Release kinetics of tritium generation in neutron irradiated biphasic $\text{Li}_2\text{TiO}_3\text{-Li}_4\text{SiO}_4$ ceramic breeder. *J. Nucl. Mater.* **2019**, *522*, 286–293. [[CrossRef](#)]
13. Yang, M.; Gong, Y.; Ran, G.; Wang, H.; Chen, R.; Huang, Z.; Shi, Q.; Chen, X.; Lu, T.; Xiao, C.; et al. Tritium release behavior of Li_4SiO_4 and $\text{Li}_4\text{SiO}_4 + 5 \text{ mol}\% \text{TiO}_2$ ceramic pebbles with small grain size. *J. Nucl. Mater.* **2019**, *514*, 284–289. [[CrossRef](#)]
14. Wang, Y.; Zhou, Q.; Xue, L.; Li, H.; Yan, Y. Synthesis of the biphasic mixture of $\text{Li}_2\text{TiO}_3\text{-Li}_4\text{SiO}_4$ and its irradiation performance. *J. Eur. Ceram. Soc.* **2016**, *36*, 4107–4113. [[CrossRef](#)]
15. Qi, Q.; Ji, B.; Gu, S.; Zhang, Y.; Zhou, H.; Luo, G.-N. Annihilation behavior of irradiation defects induced by γ -ray in biphasic tritium breeding materials $x\text{Li}_2\text{TiO}_3\text{-(1-x)}\text{Li}_4\text{SiO}_4$. *Ceram. Int.* **2021**, *47*, 434–438. [[CrossRef](#)]
16. Xiang, M.; Zhang, Y.; Zhang, Y.; Liu, S.; Liu, H.; Wang, C. Fabrication and Characterization of $\text{Li}_2\text{TiO}_3\text{-Li}_4\text{SiO}_4$ Pebbles for Tritium Breeder. *J. Fusion Energy* **2015**, *34*, 1341–1347. [[CrossRef](#)]
17. Cipa, J.; Zarins, A.; Supe, A.; Kizane, G.; Zolotarjovs, A.; Baumane, L.; Trinkler, L.; Leys, O.; Knitter, R. X-ray induced defects in advanced lithium orthosilicate pebbles with additions of lithium metatitanate. *Fusion Eng. Des.* **2019**, *143*, 10–15. [[CrossRef](#)]
18. Gong, Y.; Li, J.; Yang, S.; Yang, M.; Dang, H.; Ren, Y.; Zhang, G.; Lu, T. Improvement of crushing strength and thermal conductivity by introduction of hetero-element Al into Li_4SiO_4 . *Ceram. Int.* **2019**, *45*, 24564–24569. [[CrossRef](#)]
19. Rao, G.J.; Mazumder, R.; Bhattacharyya, S.; Chaudhuri, P. Fabrication of $\text{Li}_4\text{SiO}_4\text{-Li}_2\text{ZrO}_3$ composite pebbles using extrusion and spherodization technique with improved crush load and moisture stability. *J. Nucl. Mater.* **2019**, *514*, 321–333.
20. Hadrava, J.; Galek, V.; Stoklasa, J.; Hrbek, J.; Kunešová, K.; Bezďicka, P.; Sedlářová, I. Corrosion experiments on ceramic samples within molten salts. *J. Nucl. Eng. Radiat. Sci.* **2019**, *5*, 030910. [[CrossRef](#)]
21. Chikhray, Y.; Askerbekov, S.; Kenzhina, I.; Gordienko, Y.; Bochkov, V.; Nesterov, E.; Varlamova, N. Hydrogen isotopic effect during the graphite high-temperature corrosion in water vapours. *Int. J. Hydrog. Energy* **2019**, *44*, 29365–29370. [[CrossRef](#)]
22. Tazhibayeva, I.; Kulsartov, T.; Gordienko, Y.; Mukanova, A.; Ponkratov, Y.; Barsukov, N.; Tulubaev, E.; Platacis, E.; Kenzhin, E. Temperature dependence of the rate constant of hydrogen isotope interactions with a lithium capillary-porous system under reactor irradiation. *Fusion Eng. Des.* **2013**, *88*, 1731–1734. [[CrossRef](#)]
23. Shaimerdenov, A.; Gizatulin, S.; Dyussambayev, D.; Askerbekov, S.; Kenzhina, I. The WWR-K Reactor Experimental Base for Studies of the Tritium Release from Materials Under Irradiation. *Fusion Sci. Technol.* **2020**, *76*, 304–313. [[CrossRef](#)]
24. Tazhibayeva, I.; Ponkratov, Y.; Kulsartov, T.; Gordienko, Y.; Skakov, M.; Zaurbekova, Z.; Lyublinski, I.; Vertkov, A.; Mazzitelli, G. Results of neutron irradiation of liquid lithium saturated with deuterium. *Fusion Eng. Des.* **2017**, *117*, 194–198. [[CrossRef](#)]
25. Dang, C.; Yang, M.; Gong, Y.; Feng, L.; Wang, H.; Shi, Y. A promising tritium breeding material: Nanostructured $2\text{Li}_2\text{TiO}_3\text{-Li}_4\text{SiO}_4$ biphasic ceramic pebbles. *J. Nucl. Mater.* **2018**, *500*, 265–269. [[CrossRef](#)]
26. Kolb, M.H.; Rolli, R.; Knitter, R. Tritium adsorption/release behaviour of advanced EU breeder pebbles. *J. Nucl. Mater.* **2017**, *489*, 229–235. [[CrossRef](#)]
27. Zeng, Y.; Chen, R.; Yang, M.; Wang, H.; Guo, H.; Shi, Y. Fast fabrication of high quality $\text{Li}_2\text{TiO}_3\text{-Li}_4\text{SiO}_4$ biphasic ceramic pebbles by microwave sintering: In comparison with conventional sintering. *Ceram. Int.* **2019**, *45*, 19022–19026. [[CrossRef](#)]
28. Shlimas, D.I.; Kozlovskiy, A.L.; Zdorovets, M.V. Study of the formation effect of the cubic phase of LiTiO_2 on the structural, optical, and mechanical properties of $\text{Li}_{2\pm x}\text{Ti}_{1\pm x}\text{O}_3$ ceramics with different contents of the X component. *J. Mater. Sci. Mater. Electron.* **2021**, *32*, 7410–7422. [[CrossRef](#)]